Poincare map for scattering states

1986 J. Phys. A: Math. Gen. 19 1345

(http://iopscience.iop.org/0305-4470/19/8/016)

J. Phys. A: Math. Gen. 19 (1986) 1345-1353. Printed in Great Britain

Poincaré map for scattering states

C Jung
Fachbereich Physik, Universität Bremen, 2800 Bremen, West Germany

Received 30 July 1985

Abstract. For scattering states in classical mechanics a map is constructed, which is an analogue to the Poincaré map for bound state trajectories. Iteration of this map indicates which parts of the phase space are filled by unstable trajectories that are sensitive to small changes in the initial conditions, and which regions are filled by stable trajectories. Examples for this map are given by numerical calculations for scattering off a simple two-dimensional model potential.

1. Introduction

For Hamiltonian systems with two degrees of freedom the following question is of considerable interest: in which regions of the phase space P are the trajectories sensitive to small changes in the initial point (i.e. behave chaotically) and in which regions are they regular?

For bound states there is a method for investigating this problem, which goes back to Poincaré (1892): because the energy E is a constant in Hamiltonian systems, we restrict the considerations to the three-dimensional subset P_E of the phase space belonging to a specific value of E. In P_E we choose a two-dimensional surface S transverse to the trajectories and construct a map M (the Poincaré map) on S by the following prescription. The image of a point $x_0 \in S$ is found in this way: take the trajectory $x(t)$ through x_0 and follow it until it pierces S again in the same direction at the point x_1. Then, the point x_1 is the image point of x_0, i.e. $M(x_0) = x_1$.

For stability investigations the map M is iterated and the set $I(x_0) = \{M^n(x_0) | n \in \mathbb{N}\}$ is plotted on S. If $I(x_0)$ consists of a finite number of points only or if it is a one-dimensional set, then the trajectory through x_0 is regular (periodic or quasi-periodic respectively). If I is dense in a two-dimensional subset of S, then x_0 lies in a chaotic region. If the Poincaré plots of a system consist of invariant lines only for all energies and for all initial points, then we interpret this result as a numerical indication of a second independent conserved quantity besides the energy. For a mathematically rigorous derivation of the Poincaré map see § 7.1 in Abraham and Marsden (1978). For many examples of the utility of Poincaré plots see Lichtenberg and Lieberman (1983).

The generalisation of this idea to scattering states meets the following problem immediately. The projectile comes in from infinity, is close to the target only for a finite time and goes off to infinity again. Accordingly, any surface S is pierced only a finite number of times by a generic scattering trajectory. In this sense any generic scattering trajectory is regular, because the set of points in which it pierces S cannot be dense in a two-dimensional subset. On the other hand, this kind of regularity is

0305-4470/86/081345+09\$02.50

also fulfilled for scattering trajectories in potentials containing chaotic bound states. Therefore it does not give any hint of the existence of an analytic second integral of motion on the *whole* phase space.

The integrability of bound state systems is decided by watching the long time behaviour of trajectories that always come back into the same region of the phase space. In order to obtain a similar criterion for scattering systems, it is necessary to construct some feedback of the outgoing trajectories back into the region near the target. In § 2 a possibility for this feedback is given by cutting a neighbourhood K of the target out of the phase space and by gluing together parts of the boundary of K. This provides an automatic feedback of outgoing scattering trajectories into incoming trajectories. The geometry of this construction is explained in § 3. In § 4 numerical examples for our scattering map are given for the motion in a simple model potential. In § 5 the method is generalised to scattering in three-dimensional potentials. Section 6 contains final remarks.

2. Construction of the return map

First we consider systems with two degrees of freedom. The configuration space is a two-dimensional plane in which a projectile without internal degrees of freedom scatters off a space fixed potential. The Hamiltonian function is

$$H(x, y, p_x, p_y) = (p_x^2/2m) + (p_y^2/2m) + V(x, y) \tag{1}$$

where x, y are cartesian coordinates in the configuration space and p_x, p_y are the canonically conjugate momenta. For the moment let the support of the potential be finite, so that $V=0$ outside K_R, the circle with radius R in the configuration space. Accordingly the projectile moves along straight lines outside K_R. These straight lines can be labelled by the direction of the momentum given by the angle

$$\alpha = \tan^{-1}(p_y/p_x) \tag{2}$$

and by the impact parameter

$$b = (xp_y - yp_x)(p_x^2 + p_y^2)^{-1/2}. \tag{3}$$

Now let us look at an exact scattering trajectory with energy E hitting the target potential. For large negative times the projectile moves outside K_R along a straight line towards the potential. This incoming motion can be specified by the corresponding pair (α_i, b_i). Eventually the trajectory crosses K_R and then the projectile will stay inside K_R for some time. Even for well behaved potentials without singularities there can be a subset of values (α, b) for which the projectile gets stuck at the potential. However, those values (α, b) are an exceptional set of measure zero (see Newton 1982, ch 5.4). The generic trajectory comes out of K_R after a finite time and then the projectile moves on a straight line, again away from the potential. This outgoing asymptotic motion will be labelled by (α_f, b_f). The action of the scattering dynamics consists in connecting a given pair (α_i, b_i), which is not in the exceptional set, with the corresponding pair (α_f, b_f). Accordingly we define the scattering map M by

$$M(\alpha_i, b_i) = (\alpha_f, b_f). \tag{4}$$

M acts on incoming asymptotic states and turns them into outgoing asymptotic states of the same energy. In order to obtain an iteration, we need in addition a second map

F, which turns outgoing asymptotic states into incoming asymptotic states. Then an iteration can consist of applying M and F alternately.

In order to make a particular choice for F we use the following two reasonable restrictions.

(i) F is allowed to depend on α_f and b_f only and it must not depend on any other variables or parameters and not on the particular potential V.

(ii) If $V \equiv 0$, then the composition of M and F should be the identity map for all values of α_i and b_i, i.e. we request that

$$F \cdot M(\alpha_i, b_i) = (\alpha_i, b_i) \qquad \text{for all } (\alpha_i, b_i)$$

if $V(x, y) = 0$ for all x, y.

Under these restrictions there remains only the following choice for F: F applied to the outgoing trajectory labelled by (α, b) gives that incoming trajectory, which has the same values of α and b and E. This gives a one-to-one connection, because for any pair (α, b) there exist exactly one incoming and one outgoing asymptotic state to the fixed energy E. Therefore, in the (α, b) plane F acts like the identity and the iterated scattering map is just the iteration by the map M only. This iteration of M in the (α, b) plane is our suggestion for a scattering analogue of the Poincaré map.

3. Geometry of the feedback map F

The action of the feedback map F can be understood in the following way: first we choose a fixed value E of the energy. Because $V = 0$ outside K_R, $|\boldsymbol{p}| = \sqrt{2mE}$ on K_R. Therefore, for given energy, the state of the projectile on K_R is determined by the two angles α and φ. φ is the coordinate on the circle K_R, given by

$$\varphi = \tan^{-1}(y/x). \tag{5}$$

So, the asymptotic states of the system can be labelled by a point on a two-dimensional torus T. If $-\pi/2 < \varphi - \alpha < \pi/2 \bmod 2\pi$, then it is an outgoing trajectory and we write $(\alpha, \varphi) \in \mathrm{O}$. If $\pi/2 < \varphi - \alpha < 3\pi/2 \bmod 2\pi$, then it is an incoming state and we write $(\alpha, \varphi) \in \mathrm{I}$. For $\varphi - \alpha = \pm\pi/2$ the projectile grazes K_R tangentially. These tangential trajectories form two disjunct closed lines Γ_1 and Γ_2 on the torus T and they are the boundaries between O and I. Next, the configuration space is restricted to the disc D_R, the circle K_R and its interior. In P_E (the subset of the phase space which belongs to the energy value E) to each point of D_R a copy of the circle is attached, which gives the possible values of the direction of the momentum $\boldsymbol{p}$. Thereby a full ring U with surface T is cut out of P_E.

In the configuration space the feedback map F can be constructed in the following way: if the projectile crosses K_R from the inside to the outside in the point $\boldsymbol{q} = (x, y)$, a straight line through $\boldsymbol{q}$ is drawn in the direction of $-\boldsymbol{p}$. This line crosses K_R again at another point (x', y') which is the image of (x, y) under the map F. In the polar coordinate φ we find

$$F(\varphi) = 2\alpha + \pi - \varphi \tag{6}$$

where α is the direction of $\boldsymbol{p}$, which is conserved under F (all angles are taken modulo 2π).

On the torus T in P_E the map F can be interpreted as identification of the point $(\alpha_1, \varphi_1) \in \mathrm{O}$ with $(\alpha_2, \varphi_2) \in \mathrm{I}$ where $\alpha_1 = \alpha_2$ and $F(\varphi_1) = \varphi_2$. After this identification the energetically accessible part of the phase space for a fixed $E>0$ is a part of the interior of U together with a surface S, which is half of a torus. The identification of the points of O and I causes an automatic feedback of outgoing trajectories into incoming trajectories.

Now the scattering problem is turned into a problem with a finite configuration space and the usual procedure for the return map can be applied. For the Poincaré map the surface S is chosen. In this surface we do not use the variables α and φ but prefer α and b. This choice guarantees that the Poincaré plot is independent of the value R as long as R is so large that $V=0$ outside K_R.

4. Numerical examples

We give a few examples for the Poincaré map plotted by the prescription given in the previous sections. The following model potential is used:

$$V(x, y)=[\exp(-\xi^2)](\xi^2-B\xi^4+Cx\xi^2)(\xi^2-A^2\eta^2)^{-1} \tag{7}$$

where

$$\xi=\{[(x+A)^2+y^2]^{1/2}+[(x-A)^2+y^2]^{1/2}\}/2$$
$$\eta=\{[(x+A)^2+y^2]^{1/2}-[(x-A)^2+y^2]^{1/2}\}/2A.$$

V depends on the three free parameters A, B and C. For $C=0$ the system is separable in the elliptical coordinates (ξ, η). The distance between the two focal points of the ellipses is $2A$. For $C=0$ and $A=0$ the potential is rotationally symmetric. For $C=0$ and $B<0$ the potential is repulsive everywhere. For $B>0$ the potential is positive near the origin and negative for large distances from the origin.

This potential is not identical to zero outside some circle, but it decreases fast enough, so that we can choose $R=10$. Then the potential outside K_R does not cause any effects within the numerical accuracy. For all numerical calculations we set the mass m of the projectile to the value 1 and measure all distances and the energy in arbitrary dimensionless units.

For $C=0$ and $A=0$ the impact parameter is a conserved quantity in the scattering process. Therefore the corresponding Poincaré map is a pure twist map, where each line $b=$ constant is shifted by an angle $\theta(b)$, which is just the scattering angle. In figure 1 $\theta(b)$ is plotted for $B=1.5$ and energy $E=0.5$. For $E<1$ all points on the line $b=0$ are points of period 2. For $B>0$ there are at least two lines of fixed points. In our example in figure 1 there are two of them at $b\approx\pm1.2$.

For $C\neq0$ the system is no longer integrable and correspondingly the Poincaré map becomes a disturbed twist map. (The perturbation of twist maps is a well studied problem, see e.g. Chirikov (1979) and Greene (1979).) Figure 2 shows the iterated scattering map for $(A, B, C)=(0, 1.5, 0.2)$. Because the maps for potential (7) are symmetric under inversion in the point $(0, 0)$, only the upper half of the plot is shown. Of the fixed points at $b\approx1.2$ only two survive—one elliptic point at $\alpha=-\pi/2$ and one hyperbolic point at $\alpha=+\pi/2$. The reason is that the perturbation of the potential goes like $\cos(\varphi)$ in polar coordinates (for a perturbation like $\cos(n\varphi)$ there would be n elliptic and n hyperbolic points). In the same way for the points of order 2 at $b=0$ only one elliptic pair and one hyperbolic pair survive. For the small value 0.2 of the perturbation parameter C we do not yet see any stochastic regions in the (α, b) plane.

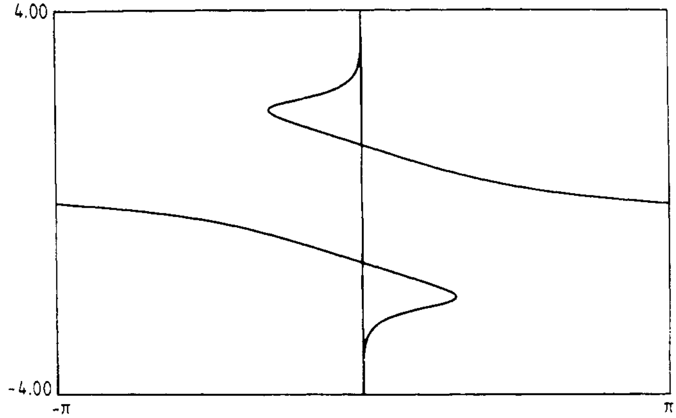

Figure 1. Classical deflection function $\theta(b)$ of the model potential (7) for the parameter values $(A, B, C) = (0, 1.5, 0)$. Energy $= 0.5$. The vertical axis gives the impact parameter. The horizontal axis gives the scattering angle.

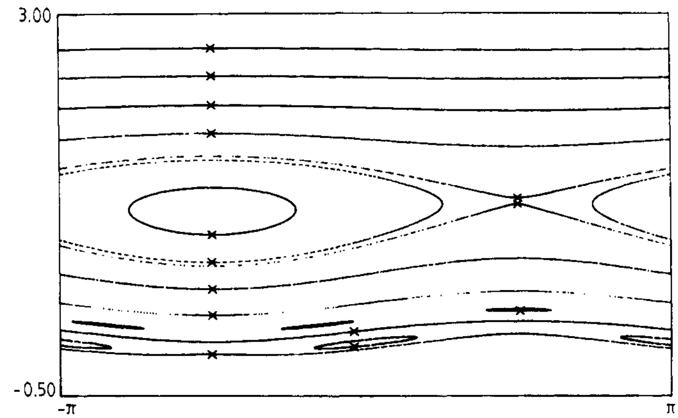

Figure 2. Poincaré plot of the model potential (7) for the parameter values $(A, B, C) = (0, 1.5, 0.2)$. Energy $= 0.5$. The vertical axis gives the impact parameter. The horizontal axis gives the angle (direction) of the momentum. The plot is symmetric under inversion at the point $(0, 0)$. Each initial point is marked by a cross.

The appearance of chaotic strips can be seen for $C = 0.4$, shown in figure 3. Along the stable and unstable manifolds of the hyperbolic point of period 2 a clearly visible chaos strip has been created. The chaos strip of the hyperbolic point of period 1 is still very narrow and in the figure it looks like a separatrix line.

Figure 4 shows the images of some lines $b = \text{constant}$ under the map M. Most image lines are quite flat and smooth. Only the line near $b = 0$ starts to grow tendrils and the image line can no longer be projected one-to-one onto its pre-image. For $C < 0.4$ all lines $b = \text{constant}$ map on quite flat lines and for C becoming greater than 0.4 more and more image lines grow tendrils of increasing complexity. Of course, for $|b| > 3$ all image lines are nearly straight because of the fast decrease of the potential for large distances from the origin. It is interesting to observe that the visible chaos in figure 3 has its origin in the region around $b \approx 0$. This connection between the beginning of tendrils in figure 4 and the appearance of chaos in figure 3 for coinciding

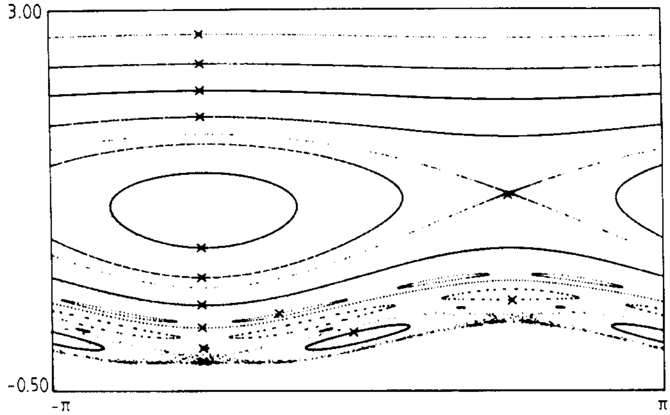

Figure 3. For explanations see figure 2. $(A, B, C) = (0, 1.5, 0.4)$.

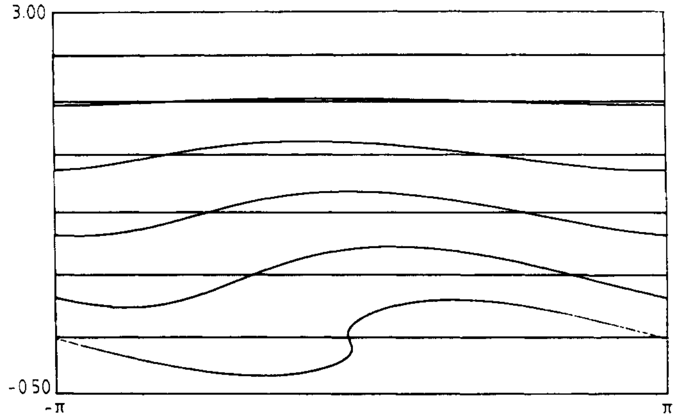

Figure 4. Several lines $b =$ constant and their images under the scattering map M. The vertical axis gives the impact parameter. The horizontal axis gives the angle (direction) of the momentum. $(A, B, C) = (0, 1.5, 0.4)$.

values of b is consistent with conclusions which MacKay and Percival (1985) have drawn from Birkhoff's theorem (Birkhoff 1920) for perturbed twist maps. They show that invariant lines going around all values of the angle are no longer existent in a region of the plane, as soon as the images of horizontal lines in this region become steeper than some limit value.

For $C = 0.7$ in figure 5 also, the hyperbolic fixed point at $b \approx 1.2$ has created a visible chaos strip. The chaos at $b \approx 0$ has already become quite large and it surrounds the islands of period 2 and the remainders of the islands of period 3.

For $C = 1$ in figure 6 there is only one large chaotic region surrounding the big island of the elliptic fixed point.

If the construction proposed in § 2 should make sense, then it must create plots consisting of invariant lines only for all integrable systems and not only for rotationally symmetric ones. Figure 7 is the Poincaré plot of potential (7) for the parameter values $(A, B, C) = (1, 3, 0)$. In this case the system is separable in elliptical coordinates and therefore it is all the more integrable. Figure 7 shows lines only and no chaotic regions. Notice that in an interval of b approximately between 0 and 1 (but outside of the two

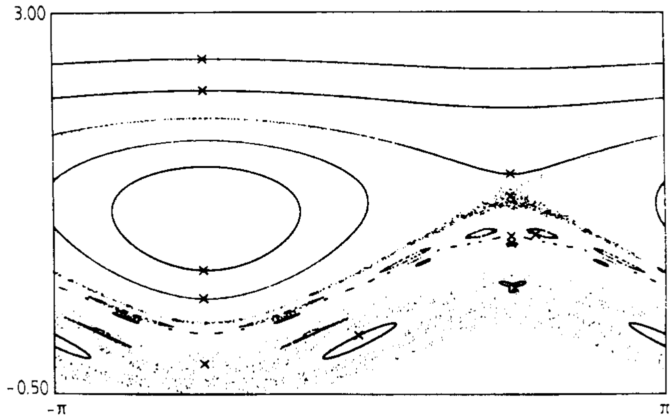

Figure 5. For explanations see figure 2. $(A, B, C) = (0, 1.5, 0.7)$.

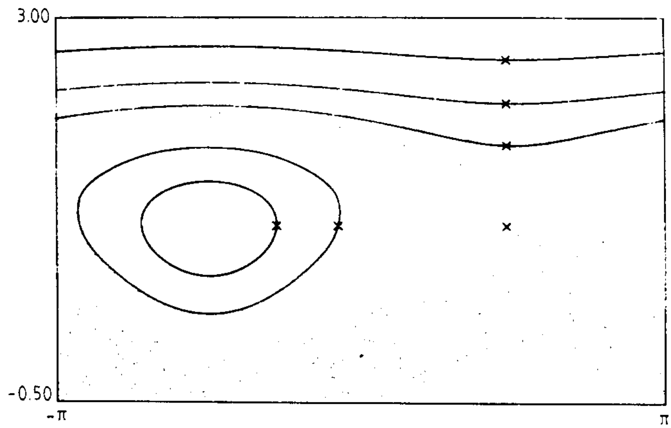

Figure 6. For explanations see figure 2. $(A, B, C) = (0, 1.5, 1)$.

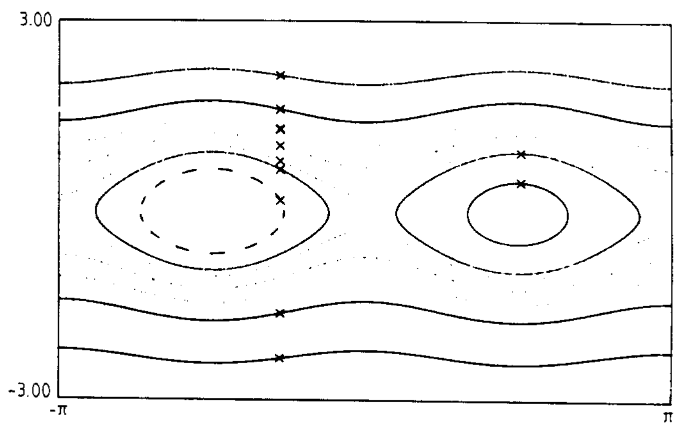

Figure 7. For explanations see figure 2. $(A, B, C) = (1, 3, 0)$.

large bubbles) any line and its counterpart for the corresponding negative value of b belong to the same initial value. In this strip in each application of M the value of b jumps from positive to negative values and back to positive values in the next step. Outside this interval the value of b remains always either positive or negative in the iteration.

For the last plot in figure 8 we have set $(A, B, C) = (1, 3, 0.5)$. Now the integrability is destroyed and accordingly we see a large chaotic region surrounding two different independent islands around elliptic fixed points and an island pair belonging to an elliptic point of period 2.

We have given examples for $E = 0.5$ only. For small E the chaos shows up for smaller values of the perturbation parameter C. For greater E the chaos becomes less and less and for $E > 1$ it is hard to find any chaotic region at all.

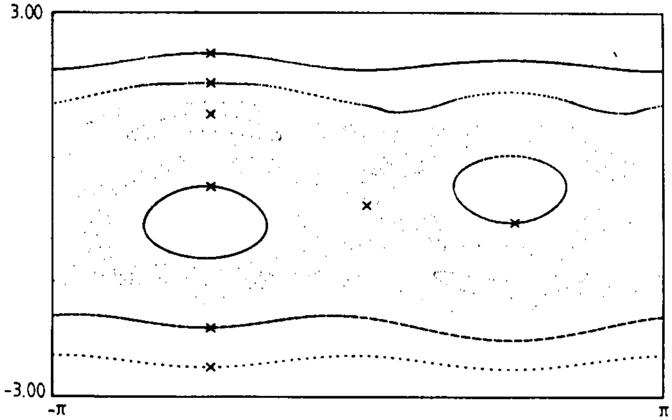

Figure 8. For explanations see figure 2. $(A, B, C) = (1, 3, 0.5)$.

5. Scattering in three-dimensional potentials

Next the method is extended to scattering in three-dimensional potentials. We can construct anything along the same pattern as in § 2. Let the potential be located around the origin of the configuration space. K_R is a two-dimensional surface of a sphere of radius R centred in the origin. R is chosen so big that V is negligible outside K_R.

For any given energy $E > 0$ each straight trajectory piercing K_R can be characterised by the direction of the momentum (given by two angles α and β) and by its two-dimensional impact parameter $\boldsymbol{b}$. For each 4-tuple $(\alpha, \beta, \boldsymbol{b})$ there is one incoming trajectory as well as one outgoing asymptotic trajectory to the energy E. These two straight trajectories are connected by the feedback map F.

By moving along the exact scattering trajectory that belongs to the incoming asymptote $(\alpha_i, \beta_i, \boldsymbol{b}_i)$, the scattering map M maps $(\alpha_i, \beta_i, \boldsymbol{b}_i)$ onto the corresponding outgoing values $(\alpha_f, \beta_f, \boldsymbol{b}_f)$. These outgoing values will be used as incoming values for the next iteration step. Thereby an iterated map is constructed in the four-dimensional $(\alpha, \beta, \boldsymbol{b})$ space. For scattering states it is the analogue to the usual four-dimensional Poincaré map for bound states of systems with three degrees of freedom.

Unfortunately, we cannot give numerical examples for these four-dimensional plots.

6. Conclusions

We have given a recipe on how to construct an iterated map for scattering states that corresponds to the usual Poincaré map for bound states. The numerical examples in § 4 suggest that our proposed construction gives reasonable results. In particular, the qualitative structure of the plots gives numerical evidence for which parameter values a second analytic integral of motion exists on the whole phase space and for which values it does not.

For the non-integrable cases the scattering map indicates which regions of the phase space are filled by trajectories that react in a regular way on small changes of the initial conditions, and which regions are filled by trajectories that react in a chaotic way on small changes of the initial conditions. Even though all scattering trajectories are regular in the sense mentioned in § 1, it might be useful to divide them into stable ones and unstable ones according to their behaviour in the iterated scattering map.

In this sense figure 8, for example, shows that, for scattering off a deformed elliptical potential, those trajectories with small impact parameter are stable which hit the ellipse near the flat side (i.e. $\alpha \approx \pm\pi/2$). In the coordinates used in equation (7) these trajectories come in along the y axis, either the positive or the negative part. Those trajectories are unstable which hit the ellipse near the most curved points (i.e. $\alpha \approx 0$ or π). These trajectories come in along the x axis, either the positive or the negative part. Trajectories with large impact parameter (i.e. those trajectories which miss the target) are always stable, an obvious result.

The method has been demonstrated on a simple model potential, which is particularly useful for the presentation of the basic ideas. However, this potential is not interesting in itself. We hope to use the method in the future to investigate the stability and the integrability of more complicated scattering systems, which are of importance for other physical problems.

Acknowledgments

The author thanks Professor P H Richter for stimulating discussions and for reading the manuscript. This work was supported financially by Stiftung Volkswagenwerk.

References

Abraham R and Marsden J E 1978 *Foundations of mechanics* (Reading, MA: Benjamin/Cummings)
Birkhoff G D 1920 *Acta Math.* **43** 1
Chirikov B V 1979 *Phys. Rep.* **52** 263
Greene J M 1979 *J. Math. Phys.* **20** 1183
Lichtenberg A J and Lieberman M A 1983 *Regular and stochastic motion* (New York: Springer)
MacKay R S and Percival I C 1985 *Commun. Math. Phys.* **98** 469
Newton R G 1982 *Scattering theory of waves and particles* 2nd edn (New York: Springer)
Poincaré H 1892 *Les methods nouvelles de la mechanique celeste* (Paris: Gauthier-Villars)